



J. Serb. Chem. Soc. 90 (11) 1415–1424 (2025)
JSCS–5462

Kinetic and equilibrium comparison of methylene blue and basic blue 41 adsorption by silica fume

SHOHRE MORTAZAVI^{1*}, MIKA SILLANPÄÄ^{2–5} and DEBAJYOTI BOSE⁶

¹Semnan University, Department of Chemical, Petroleum and Gas Engineering, Semnan, Iran,

²Saveetha School of Engineering, Saveetha Institute of Medical and Technical Sciences,

Saveetha University, Chennai, India, ³Centre of Research Impact and Outcome, Chitkara

University Institute of Engineering and Technology, Chitkara University, Punjab, India,

⁴Department of Civil Engineering, University Centre for Research & Development, Chandigarh

University, Gharuan, Mohali, Punjab, India, ⁵Sustainability Cluster, School of Advanced

Engineering, UPES, Bidholi, Dehradun, India and ⁶AI-Research Centre, School of Business,

Woxsen University, Hyderabad, Telangana, India

(Received 12 December 2024, revised 3 February, accepted 27 April 2025)

Abstract: The complex molecular structures of synthetic dyes are not easily removed from water, so it is essential to treat dye pollutants before they enter the aquatic environments. In this study, cost-effective industrial waste silica fume (SF) was used as an adsorbent to investigate the adsorption of methylene blue (MB) and basic blue 41 (BB-41). The structure of the silica fume adsorbent was characterized using the FESEM technique, which confirmed that SF has a porous structure. The adsorption of these cationic dyes was examined using kinetics models (pseudo-first-order and pseudo-second-order) and isotherm models (Langmuir, Temkin, Dubinin–Radushkevich and Freundlich), and the results obtained were compared. Based on the findings, the adsorption process of MB and BB-41 on SF followed pseudo-second-order kinetics. The adsorption of MB and BB-41 on SF followed Freundlich isotherm model. According to Langmuir isotherm data, the maximum adsorption capacity for BB-41 and MB was found to be 41.95 and 189.31 mg/g, respectively.

Keywords: isotherm; wastewater; dye removal; water treatment; industrial waste.

INTRODUCTION

Chemicals enter water through different industries, such as petrochemical, plastic, textile and cosmetic products. Millions of tons of dyes have been used for the colouring materials. Dyes and pigments have complex structures and high stability, making them difficult to remove from wastewater.¹ The toxicity of dyes threatens human health. Long-term contact with these dyes causes bleeding and

* Corresponding author. E-mail: mortazavi1398@gmail.com
<https://doi.org/10.2298/JSC241212030M>

damage to vital organs. Therefore, it is necessary to find some efficient methods to treat wastewater polluted by dyes.²

Methylene blue (MB) is not considered a toxic dye, but long-term inhalation can lead to symptoms such as breathing problems, vomiting, diarrhea and nausea. MB is commonly used for dyeing cloth, wood, and silk.^{2,3} Basic blue-41 (BB-41) is a stable mono-azo dye used in various applications from the textile industry to dyeing wool and acrylic materials. BB-41 has the potential to cause permanent damage to vital organs of humans and animals.⁴

Several methods are used to remove pollutants from wastewater, such as electrochemical degradation,⁵ membrane,⁶ adsorption^{7,8} and reverse osmosis.^{9,10} Electrochemical degradation breaks down pollutants into simpler, less harmful compounds using an electric current.⁵ The membrane filtration method removes pollutants using a membrane.⁶ The reverse osmosis (RO) is a process which uses pressure to push water through a semipermeable membrane, separating and removing contaminants from the water.⁹

Adsorption is a process in which molecules of a substance, such as dye, adhere to the surface of another material, which can be a solid or a liquid.¹¹ This mechanism is also an effective method for removing textile dyes from wastewater. Various waste materials have been investigated to remove pollutants from wastewater, such as orange and lemon peels,¹² coconut shell,¹³ palm-date stones,¹⁴ ash,¹⁵ almond shells,¹⁶ pistachio shell,⁴ Walnut shell,¹⁷ eggshell¹⁸ and steal slug.¹⁹

In the adsorption process, the determination of the rate limiting step of adsorption is one of the most important parameters. The kinetic studies are conducted to investigate the variables affecting the reaction rate.²⁰ The equilibrium isotherms of adsorption describe the interaction between the adsorbent and the adsorbate.²¹

The silica fume, a by-product of industrial waste with high purity and permeability, small particle size, high specific surface area, and low specific weight was used to eliminate MB and BB-41. Despite its low cost and easy accessibility, the previous researchers did not investigate the adsorption of cationic dyes using this adsorbent. In this research, we analysed the kinetics and equilibrium isotherms of the adsorption of MB and the BB-41 on SF from an aqueous solution to compare the optimal conditions for the adsorption of MB and BB-41 onto SF. The summary of the present study is illustrated in Fig. 1.

EXPERIMENTAL

The materials used in the study include BB-41 and MB as the synthetic dyes with specific empirical formulas and molecular weights (maximum adsorption wavelength is 610 nm for BB-41 and 665 nm for MB).

The pure SF was obtained from Lorestan Ferroalloy Company, passed through a 60-mesh sieve, and stored. The specific surface area of SF was 18 m²/g. The chemical composition and surface characteristics (determined by X-ray fluorescence) are presented in **Error! Reference source not found.**I. The maximum wavelength of the colours was determined using a

spectrophotometer (PC 1650-UV, Shimadzu, Japan). Field emission scanning electron microscopy (FESEM, JSM 6400, JEOL, Japan) was used to identify the structure of SF. **Error! Reference source not found.** shows the FESEM image of SF, and it indicates that this industrial waste has a spherical and porous structure.

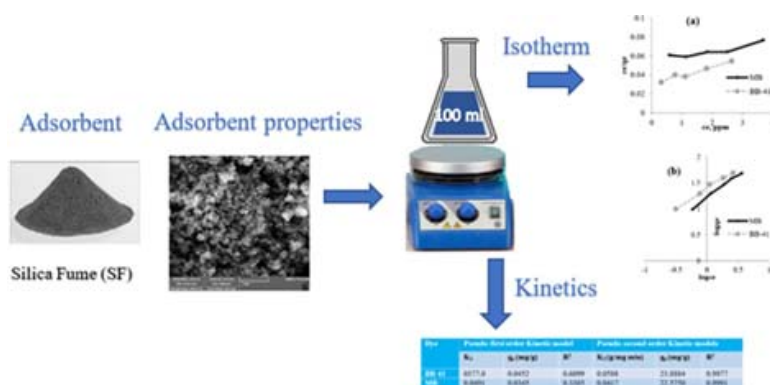


Fig. 1. Schematic of the present study in summary.

TABLE I. Chemical composition and Surface properties of SF

SiO ₂ (wt. %)	K ₂ O (wt. %)	Al ₂ O ₃ (wt. %)	Specific surface m ² /g	Density kg/m ³	Pore diameter μm
96.12	0.4	0.82	18	213	13

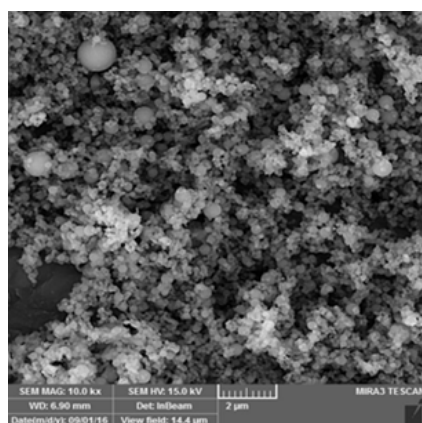


Fig. 2. FESEM structure of SF.

The 50 mg/L solution was diluted with distilled water to various concentrations in a batch system. The experiments were conducted using 0.1 to 0.5 g of adsorbent and 100 ml of solution at room temperature. The adsorption of MB and BB-41 solutions was studied using SF in the pH range of 2–11 for one hour at a speed of 300 rpm. The solution was then centrifuged and the adsorption capacity was determined using a spectrophotometer. The adsorption capacity of q (mg/g) is calculates as follows:²²

$$q_e = \frac{C_0 - C_f}{M} V \quad (1)$$

The adsorption capacity of MB and BB-41, q , is determined by measuring the initial and final concentrations of the dyes in the aqueous solution, C_0 and C_f , and calculating the adsorption capacity based on the volume of the aqueous solution, V , and the amount of SF used, M .

The Langmuir isotherm is the simplest and most common method for expressing the equilibrium of adsorption.²³

The Langmuir equation is:

$$\frac{C_e}{q_e} = \frac{1}{q_{\max} K_L} + \frac{C_e}{q_{\max}} \quad (2)$$

In the equation, q_e represent the amount of substance absorbed by SF (mg/g), C_e is the equilibrium concentration (mg/l), q_{\max} is the maximum possible adsorption capacity of MB or BB-41 (mg/g) and K_L is a constant value (l/mg).

The desirability of the adsorption process is evaluated using the dimensionless parameter R_L , known as the separation factor:

$$R_L = \frac{1}{1 + K_L C_0} \quad (3)$$

According to the value of R_L , one of the following conditions may occur:²⁴

- Irreversible adsorption occurs when R_L is zero,
- Favourable adsorption occurs when R_L is between 0 and 1 and
- $R_L = 1$ suggests a linear adsorption (C_0 is initial adsorbent (mg/l)).²⁵

The Temkin isotherm consider interactions between adsorbates and adsorbents material, while ignoring low and high concentrations. This model assumes a multi-layer adsorption process. The Temkin isotherm is represented by the following equation:²⁶

$$q_e = \frac{RT}{b_{TM}} \ln K_{TM} C_e \quad (4)$$

In this equation b_{TM} (J/mol) is related to the heat of 0.05 adsorption, R (8.314 J/(mol K)) is the universal gas constant, T is absolute temperature (K), and K_{TM} (L/mg) is Temkin model constant.

The Dubinin–Radushkevich isotherm considers the pore structure of the adsorbent for heterogeneous surfaces. This isotherm model is used to for physical or chemical adsorption. The Dubinin–Radushkevich equation is:²⁷

$$q_e = q_{m,DR} e^{-K_{DR} \epsilon_{DR}^2} \quad (5)$$

Where $q_{m,DR}$ is the maximum adsorption capacity of the Dubinin–Radushkevich model, K_{DR} is constant (mol^2/kJ^2), and ϵ_{DR} (kJ mol^{-1}) is calculated by the following equation:

$$\epsilon_{DR} = RT \ln \left(1 + \frac{1}{C_e} \right) \quad (6)$$

The Freundlich isotherm model is a mathematical relationship based on empirical observations, designed to describe non-ideal and reversible adsorption. Like the Langmuir isotherm, this model is used to quantitatively determine equilibrium and heterogeneous adsorption systems. Freundlich's linear equation is:²⁸

$$\log q_e = \log K_f + \frac{1}{n} \log C_e \quad (7)$$

The pseudo-first-order kinetic model presents the adsorption rate of a soluble substance from the environment. This kinetic model is for the physical adsorption of the solute on the adsorbent. It indicates a weak interaction between the dissolved ions and the adsorbent. The pseudo-first-order kinetic model is expressed as follows:¹⁴

$$\ln(q_e - q_t) = \ln q_e - K_1 t \quad (8)$$

The adsorption capacity at time t , q_t , and at equilibrium time, q_e , are determined and compared. The pseudo-first-order kinetic model rate constant, K_1 , describes the rate of adsorption and is calculated based on the data obtained. The pseudo-second-order model is based on the solid phase. Unlike other models, this model describes the adsorption behaviour in the entire adsorption range and shows that chemical adsorption is the slowest step and controls adsorption processes. The equation of the model is expressed as follows:²⁹

$$\frac{t}{q_t} = \frac{1}{K_2 q_e^2} + \frac{t}{q_e} \quad (9)$$

K_2 is the apparent rate constant ($\text{g}/(\text{mg min})$) which is a complex function of concentration. The width from the origin and the slope of the t/q_e line in terms of t , respectively, are obtained by the constant values of the speed and the amount of equilibrium adsorption predicted by the pseudo-second-order kinetic model.

RESULTS AND DISCUSSION

Error! Reference source not found. illustrates the impact of pH on the adsorption capacity of MB and BB-41 using SF. As the pH increased from 2 to 11, the adsorption capacity increased from 7.69 to 15.73 mg/g for MB and from 8.76 to 16.64 mg/g for BB-41. It is evident that at higher pH levels, the electrostatic force of the attraction between the dye and the adsorbent increases, resulting in the increase in adsorption capacity. The maximum adsorption capacity was observed at pH 10 for both MB and BB-41.

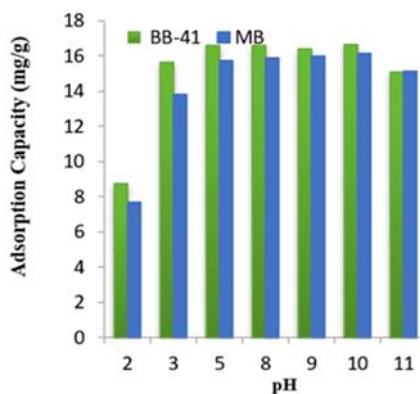


Fig. 3. Effect of pH on MB and BB-41 adsorption using SF (pH 2 to 11 at 25 °C).

To evaluate the effect of contact time on the adsorption capacity of MB and BB-41 onto SF, a series of experiments were conducted over a period of 20 to 90 min (**Error! Reference source not found.**). The results showed that the equilibrium was achieved within 30 min for MB and 20 min for BB-41.

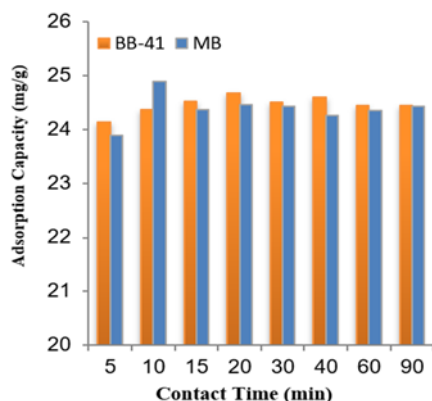


Fig. 4. Effect of contact time of MB and BB-41 on adsorption process using SF (at pH 10 and 25 °C).

Error! Reference source not found. demonstrates the effect of concentrations of MB and BB-41 on the adsorption capacity using SF at pH 10. The adsorption capacity increased with the rise in the concentrations of MB and BB-41, from 20 to 100 mg/L.

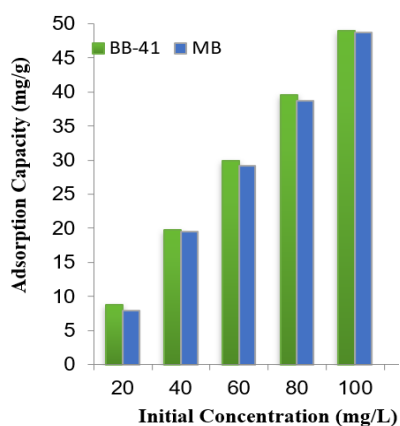


Fig. 5. Effect of initial concentration of MB and BB-41 on adsorption process using SF (at pH 10 and 25 °C).

Isotherm study

The isotherm equations were examined in order to investigate the balance of BB-41 and MB dye removal process. According to **Error! Reference source not found.**, the adsorption process of MB on SF follows the Freundlich isotherm. The maximum adsorption capacity of the Langmuir monolayer was obtained 189.31

mg/g. The adsorption process of BB-41 on SF was also fitted to the Freundlich isotherm.

The Langmuir isotherm analysis revealed that the separation factor R_L for both MB and BB-41 was found to be in the range of 0 to 1, suggesting that the adsorption process was favourable. The maximum adsorption capacity of the Langmuir monolayer for BB-41 was calculated to be 108.95 mg/g.

TABLE II. Parameters of isotherm models for removal of MB and BB-41 on SF

Model	BB-41	MB
Langmuir		
$q_{\max} / \text{mg g}^{-1}$	108.9482	189.3101
$K_L / \text{L mg}^{-1}$	0.3075	0.0970
R_L	0.0752	0.1467
R^2	0.9588	0.8473
Temkin		
b_T	134.6605	117.3272
$A_T / \text{L g}^{-1}$	4.6603	2.4972
R^2	0.9672	0.9773
Dubinin–Radushkevich		
$q_s / \text{mg g}^{-1}$	43.2213	44.3289
$\beta / \text{mol}^2 \text{kJ}^{-1}$	7.9814×10^6	3.7931×10^6
$E / \text{kJ mol}^{-1}$	0.025	0.004
R^2	0.9227	0.9443
Freundlich		
K_F	24.4589	16.3956
N	1.3059	1.1304
R^2	0.9906	0.9909

Kinetics study

Pseudo-first-order and pseudo-second-order kinetic equations were investigated for the adsorption of BB-41 and MB on SF.

As it is shown in **Error! Reference source not found.**, the adsorption of BB-41 on SF follows pseudo-second-order kinetics ($R^2 = 0.9977$). Similarly, the adsorption process of MB on SF also follows the pseudo-second-order kinetic model ($R^2 = 0.9991$).

TABLE III. Parameters of kinetic models for the adsorption of BB-41 and MB on SF

Dye	Pseudo-first order kinetic model			Pseudo-second order kinetic models		
	K_1	$q_e / \text{mg g}^{-1}$	R^2	$K_2 / \text{mg g}^{-1} \text{min}^{-1}$	$q_e / \text{mg g}^{-1}$	R^2
BB-41	0377.0	0.0452	0.6099	0.0588	23.8884	0.9977
MB	0.0491	0.0345	0.3385	0.0417	22.5750	0.9991

CONCLUSION

In this study, SF industrial waste was evaluated for its ability to remove cationic dyes BB-41 and MB from aqueous solutions in a batch adsorption process. The kinetics and the isotherm of MB and BB-41 adsorption on SF were compared. The results indicated that the adsorption kinetics for both dyes followed the pseudo-second order model, and the isotherm data were well-described by the Freundlich model. Based on the findings, FESEM images of SF revealed a spherical and porous structure for this industrial waste. Additionally, due to its non-toxic nature, accessibility, low cost and high adsorption capacity, SF can serve as a cost-effective adsorbent for eliminating coloured pollutants from wastewater. Expand the research by chemically or physically modifying SF to improve its adsorption capacity for other contaminants such as heavy metals and pharmaceuticals, allowing for a broader range of applications. To fully manage its potential, the following strategic actions are recommended:

- The future development of silica fume applications should align with circular economy principles. Efforts must focus on ensuring that silica fume is sourced sustainably, potentially through partnerships with industries that produce this byproduct.
- The comprehensive evaluations, including life cycle assessments, toxicity assessments, and ecological impact studies, are essential to ensure compliance with environmental regulations and to build public trust in this technology.
- The future research should prioritize the exploration of eco-friendly modification techniques for silica fume that enhance its adsorption capacity. Engaging local communities in projects involving silica fume for wastewater treatment can enhance industrial acceptance of its benefits.

Some further investigations are needed into the regeneration of silica fume after its use in dye removal processes. The exploring methods to effectively restore its adsorptive capabilities can significantly enhance the economic feasibility of silica.

ИЗВОД

ПОРЕЂЕЊЕ КИНЕТИКЕ И РАВНОТЕЖЕ АДОРПЦИЈЕ МЕТИЛЕНСКОГ ПЛАВОГ И BASIC BLUE-41 НА МИКРОСИЛИЦИ

HOHRE MORTAZAVI¹, MIKA SILLANPÄÄ²⁻⁵ и DEBAJYOTI BOSE⁶

¹Semnan University, Department of Chemical, Petroleum and Gas Engineering, Semnan, Iran, ²Saveetha School of Engineering, Saveetha Institute of Medical and Technical Sciences, Saveetha University, Chennai, India, ³Centre of Research Impact and Outcome, Chitkara University Institute of Engineering and Technology, Chitkara University, Punjab, India, ⁴Department of Civil Engineering, University Centre for Research & Development, Chandigarh University, Gharuan, Mohali, Punjab, India, ⁵Sustainability Cluster, School of Advanced Engineering, UPES, Bidholi, Dehradun, India и ⁶AI-Research Centre, School of Business, Woxsen University, Hyderabad, Telangana, India

Синтетичке боје сложених молекулских структура тешко се уклањају из воде, због чега је неопходно третирали загађиваче боја пре њиховог уласка у водене екосистеме. У овој студији, као адсорбенс коришћен је економичан индустријски отпад микросилика (SF) ради

испитивања адсорпције метиленског плавог (MB) и *basic blue*-41 (BB-41). Структура адсорбенса од микросилике окарактерисана је техником FESEM, којом је потврђено да SF има порозну структуру. Адсорпција ових катјонских боја испитивана је применом кинетичких модела (псеудо-првог реда и псеудо-другог реда) и изотермских модела (*Langmuir*, *Temkin*, *Dubinin–Radushkevich* и *Freundlich*), а добијени резултати су међусобно упоређени. На основу резултата, процес адсорпције MB и BB-41 на SF следио је кинетику псеудо-другог реда. Адсорпција MB и BB-41 на SF пратило се Фројндлиховим изотермским моделом. Према подацима Ленгмирове изотерме, максимални капацитет адсорпције за BB-41 и метиленског плавог је износио 41,95 mg g⁻¹, односно 189,31 mg g⁻¹.

(Примљено 12. децембра 2024, ревидирано 3. фебруара, прихваћено 27. априла 2025)

REFERENCES

1. C. Osagie, A. Othmani, S. Ghosh, A. Malloum, Z. Kashitarash Esfahani, S. Ahmadi, *J. Mater. Res. Technol.* **14** (2021) 2195 (<https://doi.org/10.1016/j.jmrt.2021.07.085>)
2. P. O. Oladoye, T. O. Ajiboye, E. O. Omotola, O. J. Oyewola, *Results Eng.* **16** (2022) 100678 (<https://doi.org/10.1016/j.rineng.2022.100678>)
3. S. T. Al-Asadi, F. F. Al-Qaim, *Research Square* **1** (2023) 1 (<https://doi.org/10.21203/rs.3.rs-2449414/v1>)
4. İ. Şentürk, M. Alzein, *Sustain. Chem. Pharm.* **16** (2020) 100254 (<https://doi.org/10.1016/j.scp.2020.100254>)
5. Y. Wang, M. Chen, C. Wang, X. Meng, W. Zhang, Z. Chen, J. Crittenden, *Chem. Eng. J.* **374** (2019) 626 (<https://doi.org/10.1016/j.cej.2019.05.217>)
6. S. Yu, H. Pang, S. Huang, H. Tang, S. Wang, M. Qiu, Z. Chen, H. Yang, G. Song, D. Fu, *Sci. Total Environ.* **800** (2021) 149662 (<https://doi.org/10.1016/j.scitotenv.2021.149662>)
7. A. Ashraf, J. Dutta, A. Farooq, M. Rafatullah, K. Pal, G. Z. Kyzas, *J. Mol. Struct.* **1309** (2024) 138225 (<https://doi.org/10.1016/j.molstruc.2024.138225>)
8. H. Bensalah, S. A. Younssi, M. Ouammou, A. Gurlo, M. F. Bekheet, *J. Environ. Chem. Eng.* **8** (2020) 103807 (<https://doi.org/10.1016/j.jece.2020.103807>)
9. R. H. Hailemariam, Y. C. Woo, M. M. Damtie, B. C. Kim, K.-D. Park, J.-S. Choi, *Adv. Colloid Interf. Sci.* **276** (2020) 102100 (<https://doi.org/10.1016/j.cis.2019.102100>)
10. C. F. Couto, A. V. Santos, M. C. S. Amaral, L. C. Lange, L. H. De Andrade, A. F. S. Foureaux, B. S. Fernandes, *J. Water Proc. Eng.* **33** (2020) 101029 (<https://doi.org/10.1016/j.jwpe.2019.101029>)
11. S. Mortazavi, E. Najafi Kani, *J. Turkish Chem. Soc., B* **6** (2023) 35 (<https://doi.org/10.58692/jotcsb.1240859>)
12. D. Ramutshatsha-Makhwedzha, A. Mavhungu, M. L. Moropeng, R. Mbaya, *Heliyon* **8** (2022) e09930 (<https://doi.org/10.1016/j.heliyon.2022.e09930>)
13. A. K. Prajapati, M. K. Monda, *J. Mol. Liq.* **307** (2020) 112949 (<https://doi.org/10.1016/j.molliq.2020.112949>)
14. M. Wakkal, B. Khiari, F. Zagrouba, *J. Taiwan Ins. Chem. Eng.* **96** (2019) 439 (<https://doi.org/10.1016/j.jtice.2018.12.014>)
15. R. Wu, A. H. Jawad, E. Kashi, S. A. Musa, Z. A. Alothman, *J. Polym. Environ.* **32** (2024) 6390 (<https://doi.org/10.1007/s10924-024-03388-1>)
16. I. Loulidi, F. Boukhelifi, M. Ouchabi, A. Amar, M. Jabri, A. Kali, S. Chraïbi, C. Hadey, F. Aziz, *Sci. World J.* **2020** (2020) 5873521 (<https://doi.org/10.1155/2020/5873521>)
17. M. K. Uddin, A. Nasar, *Sci. Rep.* **10** (2020) 7983 (<https://doi.org/10.1038/s41598-020-64745-3>)

18. S. Rajoriya, V. K. Saharan, A. S. Pundir, M. Nigam, K. Roy, *Cur. Res. Green Sust. Chem.* **4** (2021) 100180 (<https://doi.org/10.1016/j.crgsc.2021.100180>)
19. M. S. Manzar, G. Khan, P. V. Dos Santos Lins, M. Zubair, S. U. Khan, R. Selvasembian, L. Meili, N. I. Blaisi, M. Nawaz, H. A. Aziz, T. S. Kayed, *J. Mol. Liq.* **339** (2021) 116714 (<https://doi.org/10.1016/j.molliq.2021.116714>)
20. M. Benjelloun, Y. Miyah, G. A. Evrendilek, F. Zerrouq, S. Lairini, *Arabian J. Chem.* **14** (2021) 103031 (<https://doi.org/10.1016/j.arabjc.2021.103031>)
21. H. Bensalah, S. A. Younssi, M. Ouammou, A. Gurlo, M. F. Bekheet, *J. Environ. Chem. Eng.* **8** (2020) 103807 (<https://doi.org/10.1016/j.jece.2020.103807>)
22. J. Benvenuti, A. Fisch, J. H. Z. Dos Santos, M. Gutterres, *J. Environ. Chem. Eng.* **7** (2019) 103342 (<https://doi.org/10.1016/j.jece.2019.103342>)
23. K. Y. Foo, B. H. Hameed, *Chem. Eng. J.* **156** (2010) 2 (<https://doi.org/10.1016/j.cej.2009.09.013>)
24. A. Sari, Ç. Demirhan, M. Tuzen, *Chem. Eng. J.* **162** (2010) 521 (<https://doi.org/10.1016/j.cej.2010.05.054>)
25. M. A. Al-Ghouti, D. A. Da'ana, *J Hazard. Mater.* **393** (2020) 122383 (<https://doi.org/10.1016/j.jhazmat.2020.122383>)
26. M. M. Majd, V. Kordzadeh-Kermani, V. Ghalandari, A. Askari, M. Sillanpää, *Sci. Total Environ.* **812** (2022) 151334 (<https://doi.org/10.1016/j.scitotenv.2021.151334>)
27. B. S. Rath, P. S. Kumar, *Environ. Pollut.* **280** (2021) 116995 (<https://doi.org/10.1016/j.envpol.2021.116995>)
28. S. Mortazavi, M. Sillanpää, D. Bose, *Int. J. Environ. Anal. Chem.* (2024) (<https://doi.org/10.1080/03067319.2024.2426003>)
29. A. Bosacka, M. Zienkiewicz-Strzalka, A. Derylo-Marczewska, A. Chrzanowska, M. Blachnio, B. Podkościelna, *Front. Chem.* **11** (2023) 1176718 (<https://doi.org/10.3389/fchem.2023.1176718>).